# Structural Transformations during Gelatinization of Starches in Limited Water: Combined Wide- and Small-Angle X-ray Scattering Study

Rudi Vermeylen,*,† Veerle Derycke,† Jan A. Delcour,† Bart Goderis,‡ Harry Reynaers,‡ and Michel H. J. Koch§

*Laboratory of Food Chemistry, Katholieke Universiteit Leuven, Kasteelpark Arenberg 20, B-3001 Heverlee, Belgium, Molecular and Nanomaterials, Katholieke Universiteit Leuven, Celestijnenlaan 200F, B-3001 Heverlee, Belgium, and European Molecular Biology Laboratory, Hamburg Outstation, EMBL c/o DESY, Notkestrasse 85, D-22603 Hamburg, Germany*

*Received September 6, 2005; Revised Manuscript Received January 10, 2006*

Rice flour (18−25% moisture) and potato starch (20% moisture) were heated with continuous recording of the X-ray scattering during gelatinization. Rice flours displayed A-type crystallinity, which gradually decreased during gelatinization. The development of the characteristic 9 nm small-angle X-ray scattering (SAXS) peak during heating at sub-gelatinization temperatures indicated the gradual evolution into a stacked lamellar system. At higher temperatures, the crystalline and lamellar order was progressively lost. For potato starch (B-type crystallinity), no 9 nm SAXS peak was observed at ambient temperatures. Following the development of lamellar structures at sub-gelatinization temperatures, B-type crystallinity and lamellar order was lost during gelatinization. On cooling of partially gelatinized potato starch, A-type crystallinity steadily increased, but no formation of stacked lamellar structures was observed. Results were interpreted in terms of a high-temperature B- to A-type recrystallization, in which the lateral movement of double helices was accompanied by a shift along their helical axis. The latter is responsible for the inherent frustration of the lamellar stacks.

## Introduction

In plant storage organs, starch is laid down in water insoluble granules with an onion-like structure of alternating amorphous and semicrystalline shells of 120−400 nm radial thickness.[1] Within these shells, often designated as growth rings, nearly spherical blocklets have been observed.[2,3] When hydrated, the semicrystalline shells are furthermore characterized by alternating high-density and low-density lamellae, with a repeat distance of 9−10 nm.[4,5] It is generally accepted that amylopectin, which is a heavily branched α-D-glucose polymer that takes typically 70−80% of the regular starch weight, is responsible for the peculiar macromolecular structure of the granules. Indeed, the lamellar organization of the starch crystallites has been attributed to the side-chain liquid-crystalline polymer (SCLCP) behavior of amylopectin.[6] Plasticization of the amorphous amylopectin branch points (flexible spacers) enables double helices to align themselves into high-density lamellae. Moreover, double helices in the dense lamellae are packed in either a monoclinic or a hexagonal crystalline unit cell, giving rise to A- and B-type diffraction patterns, respectively.[7]

In limited moisture conditions (<32%), the 9 nm periodic lamellar structure is absent[8] due to insufficient plasticization of the flexible spacers.[7] The SCLCP concept was also used to explain differential scanning calorimetry (DSC) results obtained for starch of low moisture content, and a quite different gelatinization process was hypothesized for A- and B-type starches although no direct experimental evidence was provided.[9] In this paper, the different structural pathways of low-moisture gelatinization of potato and rice starches are demonstrated for the first time by temperature-resolved X-ray scattering.

## Experimental Section

**Materials.** Regular rice (variety Puntal) was obtained from Master Foods (Olen, Belgium), and potato tubers (Manon) were purchased from a local supermarket. Brown rice was milled and ground to pass a 250 $\mu$m sieve.[10] Starch was isolated from potato using a pronase-based procedure.[11]

**Differential Scanning Calorimetry.** DSC measurements were made on a Seiko DSC 120 (Kawasaki Kanagawa, Japan) using indium and tin as standards. Rice flour and potato starch were equilibrated in a humidifier to obtain final moisture contents of 25% and 20%, respectively. Subsequently, 5−6 mg of the specimens was accurately weighed into aluminum sample pans. These were hermetically sealed and heated at 2 °C/min from 20 to 155 °C with an empty pan as reference.

**Temperature-Resolved X-ray Scattering.** Temperature-resolved X-ray scattering experiments were performed on the ×33 camera of the EMBL in HASYLAB on the storage ring DORIS III of the Deutsches Elektronen Synchrotron (DESY) in Hamburg (Germany) at a wavelength of $\lambda = 0.15$ nm. SAXS and WAXD patterns of rice flours and potato starches were recorded with a standard data acquisition system with two delay line detectors in series.[12] Small-angle scattering data were collected in the angular range $0.03 < s < 0.35$ nm$^{-1}$ [with $s = 2\sin(\theta)/\lambda$ the modulus of the scattering vector, and $2\theta$ the scattering angle], as determined from calibration with dry calcified collagen. SAXS patterns were normalized with respect to the incident intensity of the primary beam. The WAXD patterns ($1.0 < s < 3.4$ nm$^{-1}$) were calibrated based on the position of sharp reflections of the potato starch specimen previously measured on a rotating anode wide-angle powder X-ray diffractometer (Rigaku, Tokyo, Japan) calibrated with a silicon standard.

* To whom correspondence should be addressed. Phone +32.(0)16.32.16.34. Fax +32.(0)16.32.19.97. E-mail: rudi.vermeylen@scarlet.be.
† Laboratory of Food Chemistry, Katholieke Universiteit Leuven.
‡ Molecular and Nanomaterials, Katholieke Universiteit Leuven.
§ EMBL c/o DESY.

10.1021/bm050651t CCC: $33.50 
Published on Web 03/04/2006

Samples with low moisture contents (rice flour, 18% and 25% moisture; potato starch, 20% moisture) were obtained by equilibrating in a humidifier. Flour and starch suspensions (66% moisture), for which only SAXS patterns at ambient temperature were considered in this study, were obtained by adding directly the required amount of deionized water. Samples were placed between two mica windows separated by a 1 mm thick brass spacer and inserted in a FP82HT hot stage (Mettler-Toledo, Zaventem, Belgium) through which the X-ray beam passed. After equilibration at 30 °C, samples were heated to 130 (potato starch) or 150 °C (rice flour) at a rate of 2 °C/min. In a separate experiment, a potato starch specimen (20% moisture) was heated from 30 to 130 °C at 2 °C/min, and subsequently cooled to 45 °C at the same rate. Data were collected in 30-second frames followed by a 30 s period during which the samples were protected from the X-rays by a local shutter. Each frame thus corresponds to a temperature range of 1 °C, with one frame every 2 °C. The data were normalized with respect to the incident beam intensity, and correction was made for parasitic scattering by subtracting the scattering of an empty sample holder.

**WAXD Data Treatment.** For samples that underwent a heating step only, the temperature dependence of the crystallinity was quantified by the crystallinity index (CI) procedure: crystallinity of samples with the same crystal-type was scaled between 0 and 1 by comparison with "amorphous" and "crystalline" reference spectra.[13] The diffraction patterns of the various samples measured at 30 °C served as their respective crystalline references. As samples displayed some residual crystallinity at the highest temperatures (130 or 150 °C), a recording of an amorphous potato starch sample (20% moisture, 130 °C) was used as the amorphous reference. For the rice flours, correction was made for reflections originating from crystalline amylose-lipid complexes by excluding scattering data in the range $1.37 < s < 1.56$ nm$^{-1}$ and $2.22 < s < 2.32$ nm$^{-1}$ from the CI procedure. When the 30/130/45 °C heating/cooling cycle was imposed, crystallinity of the sample at 30 (prior to heating), 130 (at the end of the heating period), and 45 °C (at the end of the cooling period) was estimated by fitting a polynomial background to the diffraction pattern. The evolution of the crystallinity between the pivotal points was evaluated with the CI procedure, which was applied separately to the heating and cooling stages. Recordings at 30 and 45 °C were taken as the respective crystalline reference spectra.

**SAXS Data Treatment.** SAXS patterns of two consecutive temperature frames were binned to improve statistics. Subsequently, the background scattering $B(s)$ superimposed on the scattering of stacked lamellar structures was subtracted using a modified Porod law[14]

$$B(s) = B_0 + B_1 s^{-4} \tag{1}$$

Here, $B_0$ is the background caused by isotropic, small-scale density fluctuations, whereas $B_1 s^{-4}$ results from large-scale heterogeneities with sharp phase boundaries. $B_1 s^{-4}$ was estimated from the recording at 30 °C, with the constraint that $B(s)$ cannot exceed $I(s)$ over the entire experimental window (0.03−0.35 nm$^{-1}$). After subtraction of $B_1 s^{-4}$, which was assumed constant in the relevant temperature range, the temperature dependence of $B_0$ was taken into account by applying the Porod eq 2 to the high-angle tail (0.18−0.35 nm$^{-1}$) of each of the SAXS patterns recorded during the heating sequence

$$\lim_{s\to\infty}\left(I(s) - \frac{B_1}{s^4}\right) = B_0 + \frac{C}{s^4} \tag{2}$$

Adjustable variables, $B_0$, a constant background, and $C$, the so-called Porod constant, were optimized using the Marquardt−Levenberg nonlinear least-squares curve fitting algorithm. Background corrected intensities were converted to linear correlation functions $K(x)$ by the Fourier cosine transformation

$$K(x) = \int (I(s) - B(s))s^2 \cos(2\pi x s)\, \mathrm{d}s \tag{3}$$

The lamellar repeat ($D$) of the stacked lamellar structure was estimated directly from the position of the first side maximum of $K(x)$. Fractional crystallinity ($\varphi$) was obtained by analysis of the autocorrelation triangle.[15] The total scattering power, or invariant $Q$, associated with the lamellar stacked system was approximated by integrating the background corrected intensities in the angular range $s$: 0.05−0.18 nm$^{-1}$:[16]

$$Q = \int (I(s) - B(s))s^2\, \mathrm{d}s \tag{4}$$

## Results

WAXD and SAXS on (1) rice flours with 18% (RF18) and 25% (RF25) moisture, and (2) potato starch at 20% moisture (PS20) were compared.

**Starch Powders at Ambient Temperature.** At ambient temperatures, rice flour, and potato starch powders were characterized by A- and B-type crystallinity, respectively (Figure 1, panels A, C, and E). SAXS showed relatively small 9 nm scattering maxima for the rice flours, with the more pronounced peak at the highest moisture content (Figure 1, panels B and D). For comparison, SAXS patterns of starch and flour suspensions (66% moisture) were recorded, and some structural parameters are listed in Table 1. Note that the positions of the maxima occurred at slightly higher angles for the low-moisture rice flours than for the suspension. Accordingly, in the 18 to 66% moisture range, the lamellar repeat distance increased from $D = 7.9$ to 8.7 nm. However, fractional crystallinity was not influenced by moisture content (Table 1). PS20 failed to reveal the characteristic 9 nm scattering maximum (Figure 1F), and the scattering pattern was modeled adequately by an equation similar to eq 1, suggesting very large structures with sharp phase boundaries,[14] such as blocklets, growth rings[17] or granules.[18]

**Temperature-Resolved WAXD.** Heating rice flours to 150 °C and potato starch to 130 °C largely reduced crystallinity (Figure 1, panels A, C and E). For RF18 and RF25, reflections at $s = 1.45$ nm$^{-1}$ and $s = 2.25$ nm$^{-1}$, typical for the V-type crystalline amylose-lipid inclusion complexes, were detected at temperatures exceeding 130 °C.[10] Up to 110 °C, PS20 displayed clear B-type diffraction patterns. Only at the highest temperatures did the remaining broad diffraction peaks reveal a weak trace of A-type crystallinity. Crystallinity of RF25 started to decrease at lower temperatures (90−110 °C) than that of RF18 (100−120 °C; Figure 2A). Apart from a small endotherm at 150 °C, DSC-analysis of rice flour did not reveal any distinguishable endothermic event (Figure 2B). Crystallinity of PS20 started to decrease markedly from 70 to 80 °C. The DSC thermogram, on the other hand, displayed the typical $M_1$ and $M_2$ endotherms, centered at 110 and 135 °C, respectively, followed by a third endotherm at 150 °C.[19] Comparison of real-time WAXD with DSC showed that, up to the peak temperature of the $M_1$-endotherm (110 °C), no obvious change in the prevailing crystal type was observed (Figure 1E). At higher temperatures, the pace of crystal melting was reduced (Figure 2A), and (very) weak A-type diffraction traces appeared.

**Temperature-Resolved SAXS.** Characteristics of the lamellar structures were derived from the SAXS patterns after subtraction of the $s^{-4}$ background indicated in Figure 1 (panels B, D, and F). In doing so, the scattering resulting from the interference between the lamellae and growth rings is neglected. As dimensions of lamellae and growth rings are largely different (see above), this approximation is legitimate, however.

Heating RF18 and RF25 had qualitatively similar effects. Linear correlation functions showed a marginal increase in the lamellar repeat distance (Figure 3), whereas $\varphi$ remained constant

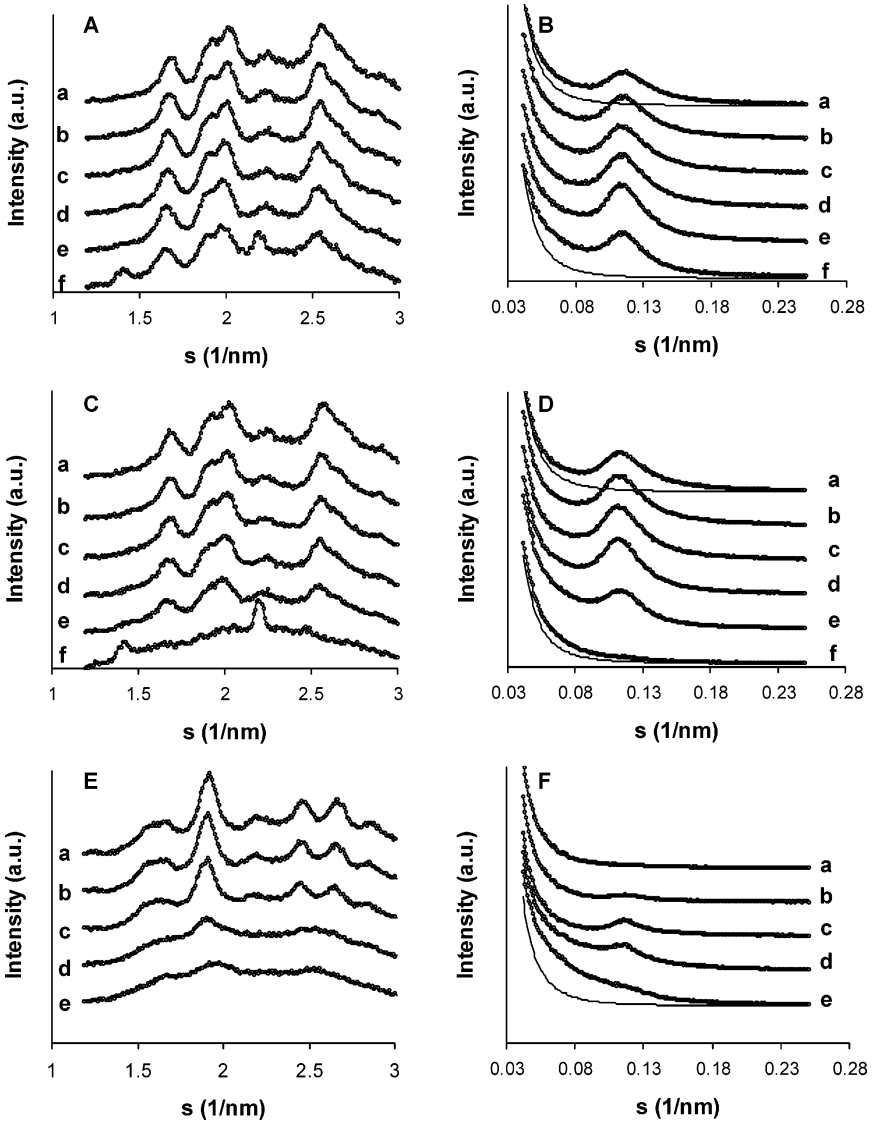


**Figure 1.** Wide-angle (A, C, E) and small-angle X-ray (B, D, F) scattering patterns of rice flour at 18% (A, B) and 25% moisture (C, D), and potato starch at 20% moisture (E, F). Scattering patterns were recorded at 30 (a), 70 (b), 90 (c), 110 (d), 130 (e), and 150 °C (f), and are shifted along the ordinate for clarity. To facilitate visual inspection, SAXS patterns B, D, F were scaled to the same $s^{-4}$ background, which is indicated for the patterns at the lowest and highest temperatures.

**Table 1.** Small-Angle X-ray Scattering Data of Rice Flour and Potato Starch at 30 °C and Various Moisture Contents

| | sample | | | | |
|---|---|---|---|---|---|
| | rice flour | | | potato starch | |
| moisture content | 66% | 25% | 18% | 66% | 20% |
| position of maximum ($s$ nm$^{-1}$) | 0.107 | 0.115 | 0.115 | 0.107 | *a* |
| $D^b$(nm) | 8.7 | 8.1 | 7.9 | 8.8 | *a* |
| $\varphi^c(-)$ | 0.73 | 0.73 | 0.73 | 0.68 | *a* |

[a] Not detected. [b] Lamellar repeat distance obtained from correlation functions. [c] Fractional lamellar crystallinity calculated by correlation function analysis.

up to 100 (RF25) and 120 °C (RF18). Furthermore, the 9 nm scattering maximum became progressively more intense (Figure 4, panels A and B) and $Q$ increased markedly.

Irrespective of the spatial arrangement of the contrasting phases, the total scattering power of an ideal two-phase system which may be embedded in a homogeneous third phase of much larger dimensions is defined by

$$Q = \alpha_s(\Delta\rho_l)^2\,\varphi(1-\varphi) \qquad (5)$$

For structures with stacked lamellae, $\alpha_s$ corresponds the volume fraction of the lamellar stacks, $\Delta\rho_l$ is the density difference between the amorphous and crystalline lamellae, and $\varphi$ is the volume fraction of the crystalline phase in the lamellar stacks.[15]

As starch crystallites are largely concentrated in the semicrystalline growth ring,[2] it is inferred from the evolution of CI that the increase in $Q$ is not due to a higher $\alpha_s$ value. Since $\varphi$ is constant, an increase in $Q$ must originate from larger $\Delta\rho_l$ values. The latter may result from double helices moving into gradually denser lamellae.

For RF18, the intensity of the 9 nm maximum increased up to 130 °C, whereupon it decreased. Along with the decreasing CI, this suggests that some lamellar crystallites melted at these elevated temperatures. Judging from $Q$ (Figure 3), the intensity due to the 9 nm lamellar repeat in RF25 increased strongly up to 80 °C. From 80 to 120 °C, the intensity at the peak position remained almost unaltered. This might indicate that, at slightly higher moisture contents (25% vs 18%), the maximal level of lamellar order achievable is reached at lower temperatures. However, as the loss of crystallinity of the rice flour at 25% moisture is more pronounced in the indicated temperature range than that of the same flour at 18% moisture, it can be speculated

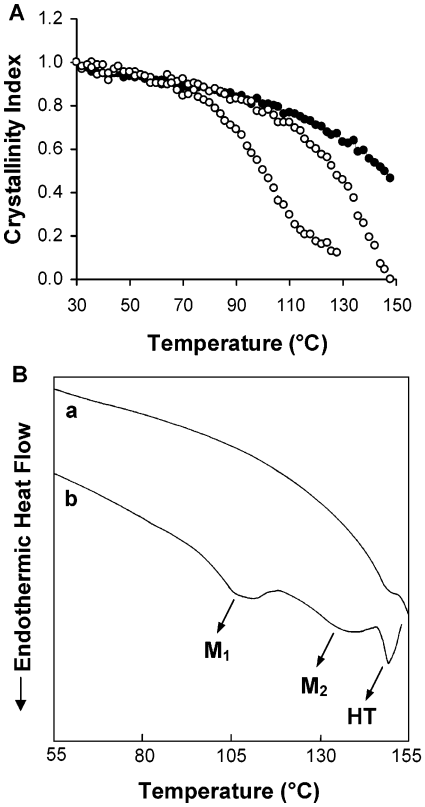


**Figure 2.** Crystallinity index as a function of temperature (A) for rice flours at 18% and 25% moisture (indicated by black and gray symbols, respectively), and potato starch at 20% moisture (open symbols). DSC thermograms (B) of rice flour at 25% moisture (a) and potato starch at 20% moisture (b). $M_1$, $M_2$ and the high temperature (HT) endotherm are indicated on the potato starch thermogram.

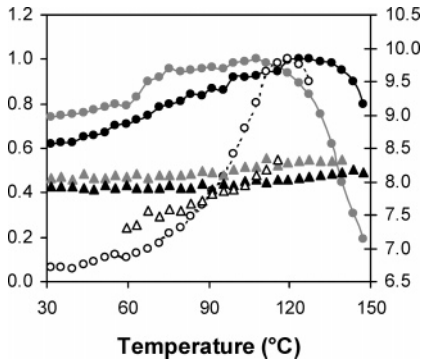


**Figure 3.** Lamellar repeat distance (*D*, triangles) and invariant (*Q* normalized to maximal *Q*, circles) of regular rice flour with 18% moisture (black symbols), regular rice flour with 25% moisture (grey symbols) and potato starch with 20% moisture (open symbols).

that, at temperatures exceeding 80 °C, the progressive transformation into a lamellar stacked structure is accompanied by a melting of the least stable lamellar crystallites. The latter would decrease $\alpha_s$ thereby counterbalancing the effect of increasing $\Delta\rho_l$ in eq 5. At higher temperatures ($T$ > 120 °C), crystal melting strongly decreased the intensity of the 9 nm scattering maximum of RF25. Only a very limited intensity increase was observed at $s < 0.08$ nm$^{-1}$ in the early stages of crystal melting. In contrast to what is deduced for the gelatinization in excess water,[20] the contrast between amorphous and semicrystalline growth rings did not increase during gelatinization in limited moisture. At 150 °C, the sharp upturn at the smallest angles indicated structural heterogeneities with characteristic dimensions exceeding 10 nm.

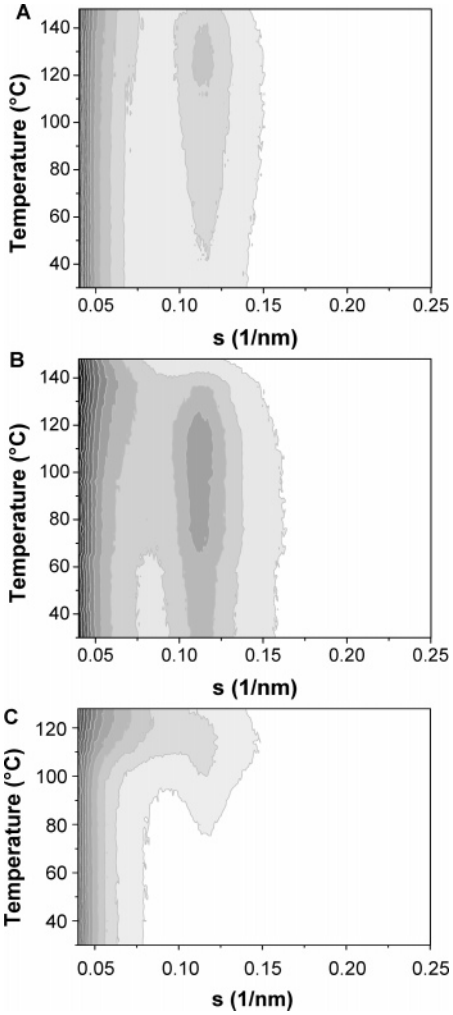


**Figure 4.** Temperature resolved SAXS patterns of rice flours at 18% (A) and 25% moisture (B), and potato starch at 20% moisture (C). Darker colors correspond to higher intensities.

PS20 developed a scattering maximum at $s = 0.117$ nm$^{-1}$ on heating from 30 to 110 °C (Figures 1F and 4C). For temperatures from 59 to 115 °C, subtraction of the $s^{-4}$ background yielded correlation functions with regular oscillating features typical for lamellar stacked systems. As the integrated intensity ($Q$) increased strongly up to 120 °C (Figure 3), results furthermore indicate the gradual formation of stacked lamellar systems; a process which occurs simultaneously with the decrease of B-type crystallinity. As the shape of the high angle tail deviated slightly from the ideal Porod behavior, the autocorrelation triangle was somewhat distorted. $\varphi$ values, which range from 0.68 at 59 °C to 0.72 at 90 °C, are thus considered less reliable. At larger distances, $K(x)$ is not influenced by limited departure from the ideal Porod behavior, and the position of the second maximum of $K(x)$ hence provided a robust estimate of the lamellar repeat distance ($D$). It seems that $D$ gradually expanded from about 7 nm at 60 °C to 8 nm at 110 °C (Figure 3).

The average lamellar characteristics were thus altered during heating of moist potato starch. Moreover, from 100 °C onward, a diffuse background developed under the 9 nm maximum (Figures 1F and 4C). As this background scattering stretched out to high angles, this effect cannot be described in terms of the lamellar stacked model.[20] The diffuse background developed at the expense of the 9 nm maximum, and this process occurred largely at temperatures corresponding to the $M_1$ endotherm. Finally at 130 °C, the 9 nm maximum was almost completely

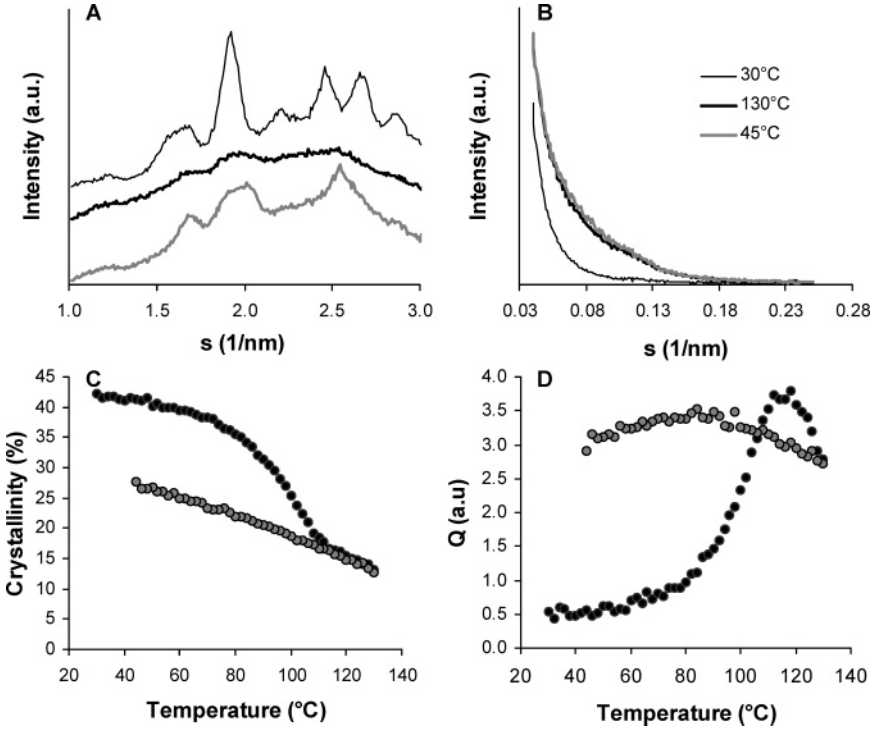


**Figure 5.** Real-time WAXD and SAXS patterns of potato starch (20% moisture) during 30/130/45 °C heating/cooling cycle. WAXD (A) and SAXS (B) patterns at 30 (thin black line), 130 (bold black line), and 45 °C (after cooling; bold gray line). Temperature dependence of WAXD based crystallinity (C) and Q, the invariant, (D) during heating (black symbols) and cooling (grey symbols).

replaced by a diffuse scattering (Figure 1F). Although the crystallinity of RF25 heated to 150 °C was close to that of PS20 at 130 °C the intensity at small angles was much higher for the latter, suggesting that melting of B-type crystallites resulted in a less homogeneous system.

**Cooling of (Partially) Gelatinized Potato Starch.** To obtain deeper insight in the gelatinization process of B-type starch, WAXD and SAXS were simultaneously recorded during the heating and subsequent controlled cooling of a potato starch specimen (20% moisture). As observed in the previous experiment, the sample appeared largely amorphous at 130 °C. On cooling, however, the typical A-type diffraction pattern emerged (Figure 5A). This pattern became gradually more intense at lower temperatures without a true crystallization temperature being observed (Figure 5C). Cooling did not restore the original 9 nm scattering maximum (Figure 5B), indicating that the melting of the original B-type crystallites irreversibly destroyed the stacked lamellar system. Although WAXD crystallinity increased linearly on cooling, $Q$ displayed a parabolic evolution (Figure 5D). This behavior can be explained by identifying the A-type crystallites with the dense phase in the starch spherulites. According to eq 5 and assuming that $\varphi < 0.50$ at 130 °C, the growth of the crystalline fraction triggers an increase in $Q$. As $Q$ is maximal when crystallites account for half of the spherulites volume, $\varphi = 0.50$ at 81 °C (Figure 5D). At lower temperatures, the further increase of A-type crystallinity and, consequently, $\varphi$, would trigger a decay of $Q$.

## Discussion

It is noted that under limited moisture conditions the 9 nm lamellar repeat was absent for PS20, even though the starch displayed appreciable crystallinity (Figure 1, panels E and F). Although the irregular packing of crystallites is expected to contribute to the small-angle scattering, the SAXS pattern ($I(s) \propto s^{-4}$) suggested the complete absence of structural heterogeneities on the nanometer-length scale for PS20. This can only be rationalized in terms of a lack of contrast between the crystallites and their amorphous surroundings in the semicrystalline growth ring.[8] Although, the above casts doubt on one of the arguments favorable to the liquid crystalline nature of amylopectin, the other arguments outlined in the 1998 paper of Waigh and co-workers[6] justify a discussion of our results based on the SCLCP concept. Accordingly, Figure 6 presents a schematic view on the gelatinization process of A- and B-type starches. The effect of increasing temperatures on the crystalline ordering, as appearing from WAXD measurements, is most conveniently visualized by an on-top view of the arrangements of double helices (bottom panels in Figure 6, parts A and B).

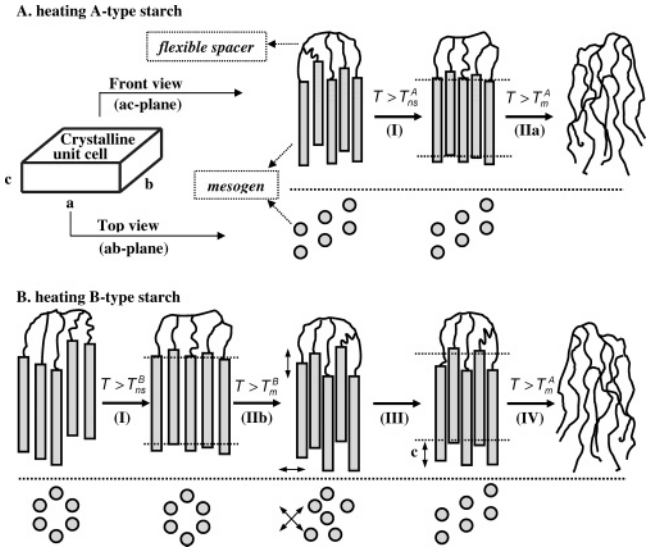


**Figure 6.** Model for the gelatinization of A-type (panel A) and B-type starch (panel B). Transitions from the nematic to the smectic phase and crystal melting at the respective characteristic temperatures, $T_{ns}$ and $T_m$, are indicated. See text for discussion.

The lamellar organization of the double helices belonging to a single amylopectin cluster is represented by an on-edge view (top panels in Figure 6, parts A and B).

**Nematic to Smectic Phase Transition.** When starch is suspended in excess water at room temperature, mesogens are aligned in dense lamellae, and the starch is in the smectic phase.[6,21] At low moisture levels (<32%), the lamellar organization is less pronounced, and the structure tends toward the nematic phase. Under these conditions, the 9 nm SAXS maximum increased upon heating. This indicated that temperatures above ambient promote a secondary transition from the nematic to the smectic phase (Figure 6, step I). Similar results have been obtained earlier with starches immersed in an excess of a less effective plasticizer (e.g., glycerol[21]). According to the SCLCP concept,[6,21] the combination of heat and plasticizer make the single-stranded parts (i.e., flexible spacers) interconnecting the amylopectin branch points sufficiently flexible to decouple the entropy maximizing mobile backbone and the double helices (i.e., mesogens). Structural heterogeneity or inhomogeneous moisture distribution would prevent the observation of a sharp phase transition temperature ($T_{ns}$). Accordingly, the gradual evolution of the intensity of the 9 nm SAXS maximum is in line with the presence of a $T_{ns}$-range. Increasing the moisture content (from 18% to 25%) affects the intensity of the 9 nm maximum in a way similar to an increase in temperature.

Higher plasticizer concentrations and higher temperature are thus interchangeable with respect to the development of stacked lamellar structures. At the level of starch crystallites, the situation seems to be more complex. Literature indicates that higher moisture contents increase WAXD crystallinity.[6,22] In line with the above, temperature increase might be expected to have a similar effect. However, we found that crystallinity of rice and potato starch remained essentially unaffected (below melting temperature). Perry and Donald,[21] on the other hand, observed a marked increase in crystallinity during heating in solvents with a lower plasticizing capacity. However, compared to dry starch powders (10−12% moisture), WAXD of these starch/glycerol suspensions reveal a reduced definition of the characteristic crystalline diffraction peaks.[21] This might indicate that glycerol has other effects than simply plasticizing the amorphous regions.

Potato starch showed a smaller tendency to become organized in lamellar stacks than rice flour. This suggests that the shorter flexible spacers in potato starch are responsible for the hampered/postponed transition from the nematic to the smectic phase.[6,23] However, the internal single-helix sections interconnecting neighboring double helices are anticipated to be longer for B-type crystallites as the mesogen density in the latter is lower than in A-type crystallites.[24] Computer simulations have actually confirmed this line of thinking.[25] Structural information on B-type starches (longer flexible spacers) thus seems not to concur with the straightforward SCLCP interpretation of SAXS data (shorter flexible spacers). However, in potato starch, lamellae are arranged in super-helical structures,[26] and possibly these complex structures reassemble less readily upon hydration than the flat lamellar structures in A-type starches.[23] Furthermore, single stranded chain fragments connecting multiple clusters were longer in B− than in A-type starches.[24,27] As these chains might correspond to the amylopectin backbone, inherent differences are envisaged in their mobility and, consequently, in the mesogens tendency toward the nematic phase.

**Starch Crystal Melting.** Higher moisture contents of the rice flours (25% vs 18%) resulted in lower melting temperatures of A-type crystallites, which is in line with earlier results.[28,29] Potato starch crystallites started to melt at much lower temperatures (70−80 °C) than the A-type crystallites of rice flours (90−110 °C), even when the moisture content of the former was lower (20% vs 25%) This suggests an intrinsically lower melting temperature of B-type amylopectin crystals.[30,31]

When temperatures exceed the crystal melting temperatures of A-type starches, the lamellar structure is disturbed (Figure 6, step IIa). The nondistinctive DSC trace of A-type starches is in line with a gradual, noncooperative melting of crystallites. Waigh and co-workers[9] suggested that double helices are stripped from the surfaces of A-type crystallites in a first, relatively slow process and that individual double helices subsequently unwind cooperatively. The melting of A-type crystals probably progressed up to the point where no double helical order is left.

For potato starch, lamellar structures kept developing at temperatures above the melting temperatures of the least stable crystallites (70−80 °C). As lamellar structures in the "molten", amorphous state have not been reported in the literature, we assume that the transition from the nematic to smectic phase and the crystal melting do not take place at the same spot. Incorporation of a single crystallite into a lamellar structure is anticipated to take place at lower temperatures than the crystal melting.

For the potato starch specimen, a biphasic $M_1/M_2$ endotherm combination was separated by an exothermic event. This has been explained in terms of the following sequence of events: (i) melting of B-type crystals, (ii) recrystallization into A-type crystallites, and (iii) melting of A-type crystallites.[19,32] The following discussions focus on the presumed melting and reorganization pathway preceding the final crystal melting process ($M_2$ endotherm; Figure 6, step IV) that is analogous to the one observed for A-type starches. The limited transition from the B- to the A-type diffraction pattern observed with real-time WAXD of potato starch thus apparently does not concur with the above-mentioned hypothesis, nor does it appear to corroborate the marked B− to A-type polymorphic phase transition deduced from post factum analysis of heated B-type lintners,[32] or heat-moisture treated potato starch.[33] Although the relatively low moisture content used in this study may have limited the B− to A-type recrystallization and shifted it to higher temperatures,[32] the recording of WAXD at high temperatures and/or without time delay might in itself have affected the level of restructuring. Indeed, on cooling of apparently largely amorphous potato starch, the A-type diffraction pattern gradually developed. The progressive crystallinity increase during cooling corresponds to both crystal growth from numerous but small A-type crystallites (or nuclei), and the gradual release of microstrains during the slow cooling of thermally agitated A-type crystals. Crystallites (or nuclei) would have been formed during the preceding heating stage. In this view, the classical idea of a high-temperature B- to A-type recrystallization, causing the exothermic event separating the $M_1$ and $M_2$ endotherms, is preserved. Moreover, the lower crystal-melting rate in the exothermic valley may be taken as a further indication of such a crystallization process (Figure 6, step III).

The rapid reformation of structures with A-type WAXD patterns suggests that the melting of B-type crystals does not involve the unwinding of double helices, but rather the movement of intact double helices out of crystalline register. Literature reports that potato starch granules,[34] or at least the granules periphery, [35] remain highly birefringent after prolonged heating at high temperatures and low moisture contents (i.e.,

heat moisture treatments). This suggests that the analogous disintegration of B-type crystallites during low-temperature gelatinization did not provoke the random orientation of A-type crystallites but rather preserved the original orientation of the double helices.

O'Sullivan and Pérez[25] suggested that the lengths of the single-stranded internal chains of a double-helix duplex are typically 4 and 6 glucose-units in B-type structures. These flexible chains give the covalently linked double helices sufficient translational freedom to allow for a favorable positioning of adjacent double helices. The reassociation of double helices into the A-type register (after the previous frustration of the B-type crystallite unit cell) includes the translation of double helices within the original lamellar plane.[7] An additional movement of double helices in their axial direction would, however, avoid the straining of the covalently linked single-stranded internal chains. Moreover, when double helices are shifted by a distance *c* along one another (with *c*, the height of the unit cell in the axial direction; Figure 6, panel B), the intimate contact between neighboring double helices is restored.[36] This implies that the proper axial translation of double helices can promote crystallization. Obviously the original lamellar structure would be lost during this melting-recrystallization process. We thus suggest that the high-temperature transition involves both a lateral and axial translation of double helices, thereby changing the crystal type and destroying the original stacked lamellar structure (Figure 6, Step IIb).

In view of the parallelism between A-type crystallization and the evolution of the total SAXS scattering during cooling of potato starch from 130 °C, it is assumed that A-type crystals are at least partially responsible for the diffuse SAXS pattern observed. Consequently, the formation of A-type crystals (or nuclei) during heating might trigger the development of a diffuse scattering at temperatures exceeding 100 °C. Alternatively, as observed in mutant potato starches,[37] disruptions of the lamellae may have repercussions on higher-order structures. Accordingly, the super-helical structures in native potato starch[26] probably break down when lamellae lose their integrity. On a macroscopic scale, heat moisture treatment preserves the granular structure of potato starch. However, in accordance with Kawabata et al.[33] large voids near the hilum were observed after heat moisture treatment.[35] Similar effects might be assumed to occur when starch is partially gelatinized. The 'melting' of the B-type crystallites and the subsequent condensation of the molten material in the granules periphery would affect the growth ring structure. Alterations in both the super-helical structure and the growth rings may markedly affect the small-angle scattering profile, and could contribute to the diffuse background observed at temperatures above 100 °C.

## Conclusions

In contrast to rice starch at ambient temperature, a stacked lamellar organization of amylopectin crystallites was not demonstrated for potato starch at limited (20%) moisture. By increasing the temperature, the 9 nm SAXS maximum gradually intensified indicating that both rice and potato starches gradually evolve from the nematic to the smectic phase. When the melting temperature of A-type crystallites is reached, crystalline and lamellar order is lost simultaneously. For potato starch, real-time WAXD during heating displayed a limited transition from B- to A-type crystallinity. On cooling, A-type crystallinity increased steadily, however. This suggests that high-temperature B- to A-type recrystallization was initiated earlier, i.e., during the heating stage. From SAXS and DSC it was deduced that the melting of B-type crystallites resulted in the gradual breakdown of lamellar structures. The loss of lamellar order was irreversible, as the characteristic 9 nm scattering maximum was not reformed during cooling.

On the nm length scale, the main effects during the heating of low-moistened B-type starches are a high-temperature recrystallization process, which involves the lateral and axial translation of double helices. These reorganizations result in the formation of A-type crystallites, which are probably radially oriented, but in contrast to the original B-type crystals, are not organized in a lamellar stacked system. The irregular packing of A-type crystallites is at least partially responsible for the development of a diffuse SAXS background at temperatures above 100 °C.

**Acknowledgment.** R.V. acknowledges the Instituut voor de Aanmoediging van Innovatie door Wetenschap en Technologie in Vlaanderen (IWT, Brussels, Belgium) for the receipt of a scholarship. B.G. is postdoctoral fellow of the Fonds voor Wetenschappelijk Onderzoek-Vlaanderen (FWO-Flanders, Brussels, Belgium). B.G., H.R., and J.A.D. thank the FWO-Flanders for continuous support and equipment. Technical assistance by Dr. E. Theunissen (Laboratory of Macromolecular Structural Chemistry, K.U.Leuven, Leuven) and Dr. G. Vandeputte and Luc Van den Ende (Laboratory of Food Chemistry, K.U.Leuven, Leuven, Belgium) is gratefully appreciated.

## References and Notes

(1) French, D. In *Starch Chemistry and Technology*; Whistler, R. L., BeMiller, J. N., Paschall, J. F., Eds.; Academic Press: San Diego, CA, 1984; pp 183−247.
(2) Gallant, D. J.; Bouchet, B.; Baldwin, P. M. *Carbohydr. Polym.* **1997**, *32*, 177−191.
(3) Ridout, M. J.; Parker, M. L.; Hedley, C. L.; Bogracheva, T. Y.; Morris, V. J. *Biomacromolecules* **2004**, *5*, 1519−1527.
(4) Oostergetel, G. T.; van Bruggen, E. F. J. *Starch/Staerke* **1989**, *41*, 331−335.
(5) Putaux, J. L.; Molina-Boisseau, S.; Momaur, T.; Dufresne, A. *Biomacromolecules* **2003**, *4*, 1198−1202.
(6) Waigh, T. A.; Perry, P.; Riekel, C.; Gidley, M. J.; Donald, A. M. *Macromolecules* **1998**, *31*, 7980−7984.
(7) Imberty, A.; Buléon, A.; Tran, V.; Pérez, S. *Starch/Staerke* **1991**, *43*, 375−384.
(8) Sterling, C. *J. Polym. Sci.* **1962**, *56*, S10−S12.
(9) Waigh, T. A.; Gidley, M. J.; Komanshek, B. U.; Donald, A. M. *Carbohydr. Res.* **2000**, *328*, 165−176.
(10) Derycke, V.; Vandeputte, G. E.; Vermeylen, R.; De Man, W.; Goderis, B.; Koch, M. H. J.; Delcour, J. A. *J. Cereal Sci.* **2005**, *42*, 334−343.
(11) Morrison, W. R.; Milligan, T. P.; Azudin, M. N. *J. Cereal Sci.* **1984**, *2*, 257−271.
(12) Rapp, G.; Gabriel, A.; Dosière, M.; Koch, M. H. J. *Nucl. Instrum. Methods* **1995**, *A357*, 178−182.
(13) Wakelin, J. H.; Virgil, H. S.; Crystal, E. *J. Appl. Phys.* **1959**, *30*, 1954−1662.
(14) Porod, G. In *Small-angle X-ray scattering*; Glatter, O., Kratky, O., Eds.; Academic Press: London, U.K., 1982; pp 17−52.
(15) Goderis, B.; Reynaers, H.; Koch, M. H. J.; Mathot, V. B. F. *J. Polym. Sci. B, Polym. Phys.* **1999**, *37*, 1715−1738.
(16) Jacobs, H.; Mischenko, S.; Koch, M. H. J.; Eerlingen, R. C.; Delcour, J. A.; Reynaers, H. *Carbohydr. Res.* **1998**, *306*, 1−10.
(17) Donald, A. M. *Cereal Chem.* **2001**, *78*, 307−314.
(18) Suzuki, T.; Chiba, A.; Yano, T. *Carbohydr. Polym.* **1997**, *34*, 357−363.
(19) Thiewes, H. J.; Steeneken, P. A. M. *Carbohydr. Polym.* **1997**, *32*, 123−130.
(20) Cameron, R. E.; Donald, A. M. *Polymer* **1992**, *33*, 2628−2636.
(21) Perry, P. A.; Donald, A. M. *Biomacromolecules* **2000**, *1*, 424−432.

(22) Buléon, A.; Bizot, H.; Delage, M. M.; Pontoire, B. *Carbohydr. Polym.* **1987**, *7*, 461−482.
(23) Daniels, D. R.; Donald, A. M. *Biopolymers* **2003**, *69*, 165−175.
(24) Gérard, C.; Planchot, V.; Colonna, P.; Bertoft, E. *Carbohydr. Res.* **2000**, *326*, 130−144.
(25) O′Sullivan, A. C.; Pérez, S. *Biopolymers* **1999**, *50*, 381−390.
(26) Oostergetel, G. T.; van Bruggen, E. F. J. *Carbohydr. Polym.* **1993**, *21*, 7−12.
(27) Bertoft, E. *Carbohydr. Polym.* **2004**, *57*, 211−224.
(28) Donovan, J. W. *Biopolymers* **1979**, *18*, 263−275.
(29) Le Bail, P.; Bizot, H.; Ollivon, M.; Keller, G.; Bourgaux, C.; Buléon, A. *Biopolymers* **1999**, *50*, 99−110.
(30) Whittam, M. A.; Noel, T. R.; Ring, S. G. *Int. J. Biol. Macromol.* **1990**, *12*, 359−362.
(31) Crochet, P.; Beauxis-Lagrave, T.; Noel, T. R.; Parker, R.; Ring, S. R. *Carbohydr. Res.* **2005**, *340*, 107−113.
(32) Le Bail, P.; Bizot, H.; Buléon, A. *Carbohydr. Polym.* **1993**, *21*, 99−104.
(33) Kawabata, A.; Takase, N.; Miyoshi, E.; Sawayama, S.; Kimura, T.; Kudo, K. *Starch/Staerke* **1994**, *46*, 463−469.
(34) Eerlingen, R. C.; Jacobs, H.; Van Win, H.; Delcour, J. A. *J. Therm. Anal.* **1996**, *47*, 1229−1246.
(35) Vermeylen, R.; Goderis, B.; Delcour, J. A. *Carbohydr. Polym.* **2006**, accepted for publication.
(36) Pérez, S.; Imberty, A.; Scaringe, P. In *Computer modeling of carbohydrate molecules*; French, A. D., Brady, J. W., Eds.; American Chemical Society: Washington, DC, 1990; pp 281−299.
(37) Blennow, A.; Hansen, M.; Schulz, A.; Jørgensen, K.; Donald, A. M.; Sanderson, J. *J. Struct. Biol.* **2003**, *143*, 229−241.

BM050651T